SCIENTIFIC REPORTS

OPEN

SUBJECT AREAS:
BIOMEDICAL MATERIALS
MATERIALS SCIENCE

Received
19 August 2014

Accepted
8 December 2014

Published
14 January 2015

Correspondence and requests for materials should be addressed to Y.D. (yrduan@shsmu.edu.cn; dyorong@163.com) or H.G. (hcgu@sjtu.edu.cn)

* These authors contributed equally to this work.

Low toxicity and long circulation time of Polyampholyte-coated magnetic nanoparticles for blood pool contrast agents

Qi Wang[1,2]*, Ming Shen[1]*, Tao Zhao[1], Yuanyuan Xu[1], Jiang Lin[3], Yourong Duan[1] & Hongchen Gu[1]

[1]State Key Laboratory of Oncogenes and Related Genes, School of Biomedical Engineering, Shanghai Jiao Tong University, Shanghai 200032, China, [2]Key Laboratory of Drug Targeting and Novel Drug Delivery Systems, Ministry of Education, West China School of Pharmacy, Sichuan University, Chengdu 610041, China, [3]Department of Radiology, Shanghai Zhongshan Hospital, Shanghai Medical College, Fudan University, Shanghai 200032, China.

Polyampholyte-coated (poly(acrylic acid) (PAA)-co-3-(diethylamino)-propylamine (DEAPA)) magnetite nanoparticles (PAMNPs) have been prepared as contrasting agent used in magnetic resonance imaging (MRI). Excellent biocompatibility is required for contrasting agents used in high-resolution magnetic resonance angiography. To evaluate the biocompatibility of PAMNPs, some experiments have been conducted. The hemolysis, plasma recalcification, dynamic blood clotting, prothrombin time, inflammatory cytokine release and complement system activation assays were carried out to investigate the hemocompatibility. To evaluate the toxicity to vessel, MTT test and vascular irritation tests were conducted. Tissue toxicity test was also performed to investigate the biocompability *in vivo*. We also looked into the biodistribution. The results showed that PAMNPs at the working concentration (0.138 mM) present similar hemocompatibility with negative control, thus have no significant effect to vessels. PAMNPs were mainly distributed in the liver and the blood. The circulation time in blood was considerably long, with the half-time of 3.77 h in plasma. This property is advantageous for PAMNPs' use in angiography. PAMNPs could be metabolized rapidly in mice and were not observed to cause any toxic or adverse effect. In short, these results suggest that the PAMNPs have great potential to serve as safe contrast agents in magnetic resonance imaging (MRI).

Magnetite nanoparticles have been widely used in biomedical applications, especially as contrast agents in magnetic resonance imaging (MRI)[1–13]. Various kinds of magnetite nanoparticles with high r1 relaxivity and low ratio of r2/r1 were explored for contrast-enhanced magnetic resonance angiography (MRA)[13–19]. However, the disadvantages of magnetite nanoparticles, including their high surface energy, which resulted in aggregation.

In order to overcome the aggregation of nanoparticles caused by the high surface energy, dextran, carboxydextran, and citric acid with good biocompatibilities have been used for modifying ultrasmall superparamagnetic iron oxide (USPIO)[20–23]. However, previous efforts involved complicated and tedious preparation process. In our previous research, a new kind of polyampholyte-coated (poly(acrylic acid) (PAA)-co-3-(diethylamino)–propylamine (DEAPA)) magnetite nanoparticles (PAMNPs) had been synthesized[24–26]. The preparation process is simple, time-saving and low energy-consuming. This nanoparticles had well-controlled size, high crytallinity and high water solubility. The MRA evaluation indicated PAMNPs have long blood circulation time and showed high efficiency for MRA first-pass and equilibrium imaging[24].

Biocompatibility refers to the ability of a biomaterial to perform with an appropriate host response in a specific situation[27–30]. It is an important property that blood-contacting biomaterials should possess for clinical use[31–33]. We preliminarily focus on the evaluation of hemocompatibility of PAMNPs. Furthermore, toxicity to vessel and tissue have also been discussed. The results showed that the PAMNPs have unexceptionable hemocompatibility, as under our working concentration, the PAMNPs show any toxicity to organs or vessels. This is because the PAMNPs could be eliminated by the liver and other organs *in vivo*, thus causing little toxicity to the body. The

blood circulation time is also significantly long as contrast agents in MRI. All, these results provide strong evidence for clinical therapeutic benefits. Further studies will be conducted in the future.

Methods

Materials. The tumor necrosis factor TNF-α and interleukin IL-1β ELISA test kits were purchased from the Beyotime Institute of Biotechnology (Shanghai, China). Complement C_3 assay kit was purchased from NanJing JianCheng Bioengineering Institute (NanJing, China).

HUVEC (human umbilical vascular endothelial cells) and THP-1 cells (human monocytic leukemia cell line), were obtained from the Type Culture Collection of the Chinese Academy of Sciences, Shanghai, China.

Preparation of polyampholyte-coated (poly (acrylic acid) (PAA)- co-3-(diethylamino)-propylamine (DEAPA)) magnetite nanoparticles (PAMNPs). The methods were carried out in accordance with the approved guidelines. PAMNPs were synthesized based on the poly(acylic acid) (PAA)-coated magnetite nanoparticles, which was synthesized by the microwave polyol method. Then the surface was modified into zwitterionic via a well-established EDC/NHS chemistry[24,25].

FTIR readings were measured using a Nicolet NEXUS-670 Fourier Transform Infrared Spectrometer. Transmission electron microscopy (TEM, JEOL 2010F) observation was used for observing the size and morphology of the PAMNPs. Acid-base titration was used to determine the content of superficial carboxyl groups. The ζ-potential was measured on Zetasizer Nano (Malvern) 134 and Mettler Toledo Seven Easy S20 pH meter.

Hemocompatibility of PAMNPs. *Hemolysis.* Fresh rabbit whole blood containing sodium citrate (3.8 wt%) in a ratio of 9 : 1 was diluted with saline (8 mL rabbit blood: 10 mL saline). PAMNPs was suspended in 0.9% NaCl to different concentrations[34].

The solutions of PAMNPs were incubated for 1 h at 37°C in a shaking water bath. Diluted blood (0.2 mL) was added into the solutions and incubated for 1 h. Positive and negative controls were produced by adding 0.2 mL of diluted blood to 10 mL of distilled water or saline. The release of hemoglobin was determined after centrifugation at 3000 rpm for 5 min by photometric analysis of the supernatant at 545 nm. The same concentrations of the PAMNPs had been treated according to the same process, and used as the zero setting. The hemolysis ratio (HR) was calculated from the optical density (OD) data:

$$\mathrm{HR}(\%) = 100\left(\mathrm{OD}_{\text{test sample}} - \mathrm{OD}_{\text{negative control}}\right) / \left(\mathrm{OD}_{\text{positive control}} - \mathrm{OD}_{\text{negative control}}\right)$$

All data were calculated based on the average of three replicates.

Plasma recalcification time (PRT). Platelet poor plasma (PPP) was prepared by centrifuging the whole blood (containing 3.8 wt% citrate acid solution, blood/citrate acid = 9 : 1) at 3000 rpm for 10 min[35].

PAMNPs were dissolved in 0.025 M $CaCl_2$ to different concentrations, 100 μL of the resulting solutions were added into a siliconized glass tube. 100 μL of PPP preheated to 37°C were added into the samples. After 50~80 s, the tube was tilted every 1 to 2 s to observe the clotting time. Glass tube was taken as the positive control, and siliconized glass tube as the negative control.

Quantification of whole blood clotting time. PAMNPs were dissolved in $CaCl_2$ (0.2 mol/L) to different concentrations, 0.025 mL of the solutions were added into a siliconized glass tube. Similarly, glass tube served as positive control, siliconized glass tube as negative control[36–38].

Test tubes were placed in a thermostat at 37°C for 5 min. 0.2 mL of ACD whole blood containing 3.8 wt% citrate acid solutions (blood/citrate acid = 9 : 1) were then added into the tubes. At specific time points, 50 mL of distilled water was gently added into the tubes. The OD of the supernatant was determined at 545 nm wavelength using a spectrophotometer. The relative absorbance of 0.2 mL ACD whole blood diluted by 50 mL distilled water was assumed to be 100. The same concentrations of the PAMNPs had been treated according to the same process, and used as zero setting. The blood clotting index (BCI) was quantified by the ratio of the absorbance of blood contacted with the sample to that of diluted ACD whole blood. The relative clotting time of each sample was obtained from the OD versus time plots.

Prothrombin time (PT). Rabbit brain extracts (RBE) was prepared firstly. 0.3 g of dried rabbit brain powder,4.9 ml of normal saline, and 0.1 ml of 0.1 mol/L sodium oxalate were vibrated in 45°C water bath. 45 min later, they were centrifuged at 3500 r/min × 5 min to get the supernatant[38,39].

PAMNPs were dissolved in 0.025 M $CaCl_2$ to different concentrations, 100 μL of the resulting solutions were added into a siliconized glass tube. 100 μL of PPP (described in Plasma recalcification time (PRT)) and 100 μL of RBE preheated to 37°C were added into the samples. After 50~80 s, the tube was tilted every 1 to 2 s to observe the clotting time. 0.9% NaCl had been used as the negative control. Prothrombin time of the sample was compared with that of negative control and PT ratio (PTR) was derived.

Inflammatory cytokine release and Complement system activation. THP-1 cells were incubated into 96-well plates and differentiated into adherent macrophages by 25 $ngmL^{-1}$ PMA (phorbol 12-myristate 13-acetate). 72 h later, the growth medium was replaced with the PAMNPs with different concentrations. 6.4% phenol solution in medium was taken as a positive control. After 24 h, the concentrations of tumor necrosis factor TNF-α and interleukin IL-1β were determined using ELISA. All of the experiments were performed in triplicate.

Fresh rabbit blood was incubated for 1 h at 37°C, the clotted blood was centrifuged at 1000 g for 20 min to separate the serum. The serum was incubated with PAMNPs to different concentration. PBS was tested as the negative control. The positive control was zymosan (Sigma) at the concentration of 2.5 mg/ml. After incubation for 1 h at 37°C, the concentrations of complement component C_3 in the serum after incubation were measured with immunoturbidimetry according to the manufacturer's instructions.

Toxicity to vessel. *Vascular irritation test.* PAMNPs were diluted to 138 mM with 0.9% NaCl. 0.5 ml of this PAMNPs solution had been injected into one side ear vein of the rabbit, and the other side was 0.9% NaCl. Three days later, the ear vein and the surrounding tissues which were 1 cm and 5 cm away from the injection point had been harvested, fixed by 4% paraformaldehyde, HE stained and checked by microscope[39,40].

Vascular endothelial cells cytotoxicity. PAMNPs were dissolved in DMEM to different concentrations. DMEM culture medium was used as negative control. HUVEC cells in 96-well cell culture plates were incubated with these samples for 24 and 48 h and detected by MTT (3-(4,5-Dimethylthiazol-2-yl)-2,5-diphenyltetrazolium bromide, 5 mg/mL) method. The same concentrations of the PAMNPs without the HUVEC cells had been treated according to the same process, and used as zero setting. The cell viability was calculated from the OD data of the test sample and negative control using the following equation. All experiments were carried out in triplicate. The data was expressed in mean ± S.D.

$$\text{Relative activity}(\%) = 100 * \mathrm{OD}_{\text{test sample}} / \mathrm{OD}_{\text{negative control}}$$

Toxicity to tissue. *Tissue distribution of PAMNPs.* 6 groups of 6 mice each were injected with 0.2 ml of PAMNPs (138 mM) respectively through the caudal vein. The eyeballs were extracted and blood was drawn at 0, 5, 15, 30, 60, 120, 180 and 300 min respectively after injection, after which the animals were put to death immediately and tissues of heart, liver, spleen, lungs, kidneys were taken. The blood was centrifuged (5000 r/min × 10 min) and the plasma was collected. The visceral organs were rinsed of residual blood, blotted up, weighed and stored at −20°C for assay.

Fe content was determined by the following method. The tissue was precisely weighed, mixed acids (nitric acid : perchloric acid = 4 : 1) were added into it at the ratio of 1 g tissue/100 ml, homogenate was then prepared and soak overnight. 10 ml of the homogenate fluid was injected into a round flask, and heated from 79°C to 280°C with temperature rising gradually, then maintained at 280°C until dried. After cooling, 4 ml of 1.5% hydrochloric acid was added to dissolve the residue. The content of Fe element was then determined with an atomic absorption spectrophotometer[40,41].

The curve of concentrations of Fe element in plasma and was plotted various organs against time. The data was inputted into DAS software for processing and the pharmacokinetics constant was calculated.

Tissue slice inspection. The toxicity in vivo was investigated using mice subject. 0.2 ml PAMNPs solution (diluted to 0.138 mM and 138 mM with 0.9% NaCl) was injected into the tail vein every other day. 14 days later, the mice were killed, the organs (heart, liver, spleen, lung, kidney) were harvested, fixed by 4% Paraformaldehyde, HE stained and checked by microscope[41,42].

Statistical analysis. Statistical analysis was performed using SPSS 10.0 software. Descriptive data was expressed as the arithmetic mean value plus or minus the standard deviation. Statistics were performed for all comparisons. All quantitative results were obtained from at least triplicate samples. The methods were performed in accordance with the guidelines and regulations of Shanghai Cancer Institute, Renji Hospital, School of Medicine, Shanghai Jiao Tong University. The experiments were approved by the ethics committee of the Shanghai Cancer Institute, Renji Hospital, School of Medicine, Shanghai Jiao Tong University.

Ethical approval. Ethical approval was given by the medical ethics committee.

Results and discussion

Characteristics of PAMNPs. As showed in Figure 1(A), reaction of polyacrylic acid (PAA)-coated magnetite nanoparticles (PM) and 3-(diethylamino)propylamine (DEAPA) catalyzed by EDC/NHS had formed a zwitterionic structure[24–26]. This property led high water solubility of PAMNPs and would overcome the aggregation of magnetic nanoparticles.

TEM images and the corresponding size distributions of PAMNPs were presented in Figure 1(B) and (C). The TEM picture showed that the PAMNPs had well-controlled size and were of uniform spherical shape. The average size of PAMNPs was 4.5 ± 1.4 nm. Isoelectric

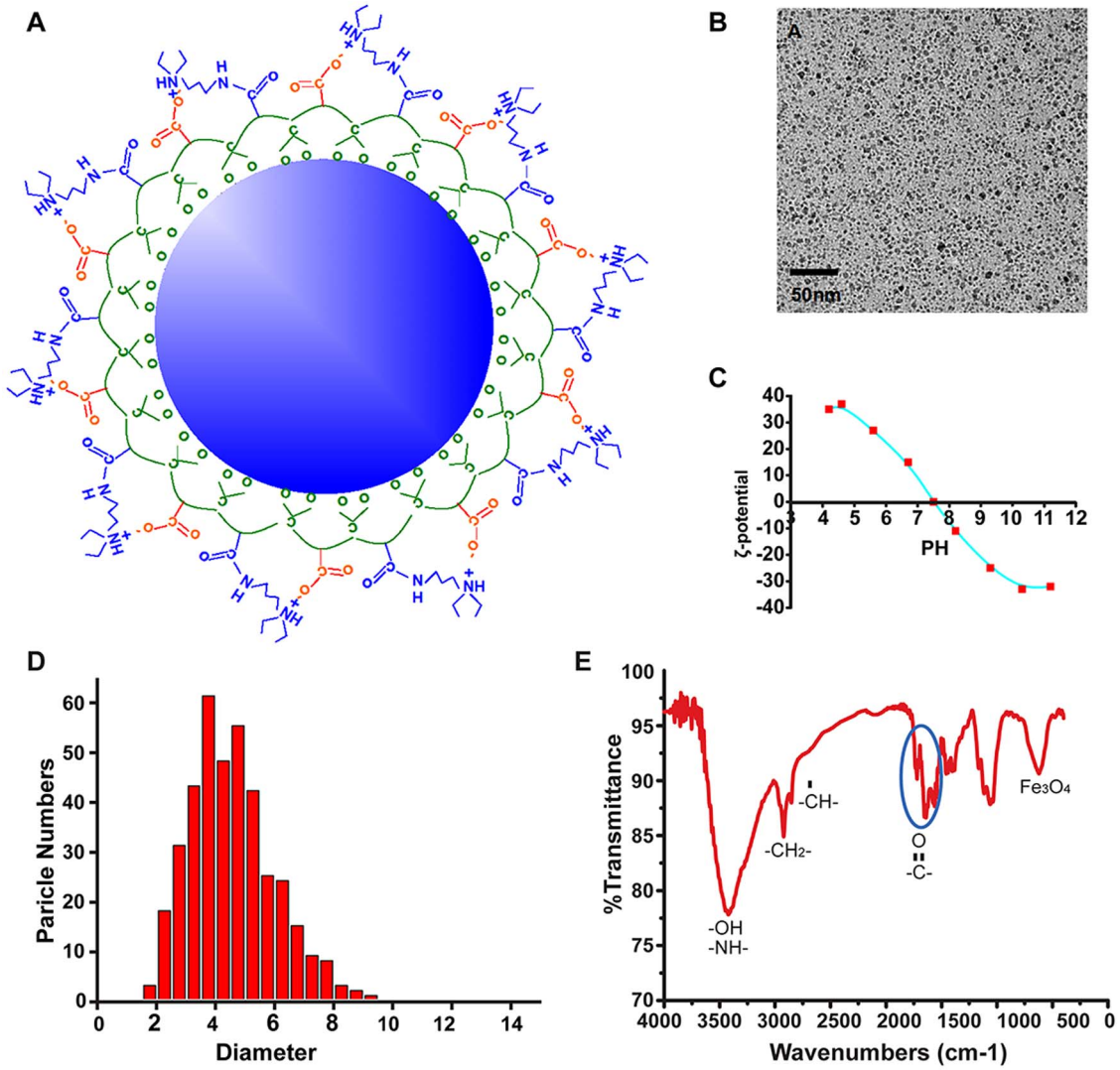

Figure 1 | (A): Structural Features of PAA-Coated Magnetite Nanoparticles (PAMNPs). The PAMNPs exist as zwitterionic structure which would improve on the aggregation property. Characteristics of PAMNPs (B):TEM image; (C): size distributions; (D): ζ-potential; (E): FTIR spectra). The average size of PAMNPs is small (4.5 ± 1.4 nm), and ζ-potential is 7.5.

point obtained from zeta potential measurement in Figure 1(D) for PAMNPs was 7.5. The characteristic absorption peak of Fe_3O_4 was found to be at 621 cm^{-1} (Figure 2E). Infrared absorption peaks of carbonyl groups were found to be at 1577 cm^{-1} (Amide bond), 1639 cm^{-1} and 1720 cm^{-1} (polyacrylic acid). stretching vibration of hydroxyl showed up as a strong broad peak from about 3000–3700 cm^{-1} and the stretching vibration of amine was not observed. Methylene (2922 cm^{-1}) and Methine (2852 cm^{-1}) was found in the spectrum. Methyl absorption peak appeared as a shoulder peak at 2947 cm^{-1}.

It implied that half of the carboxyl groups on PAA was transformed into amino groups via a well-established EDC/NHS chemistry.

Hemocompatibility of PAMNPs. Biocompatibility refers to the ability of a biomaterial to perform with an appropriate host response n a specific situation. This is an important trait for blood-contacting biomaterials adopted in clinical use.

Hemolysis. Hemolytic reaction caused by preparations as drugs includes immune hemolysis and non-immune hemolysis[42]. According to the guide for evaluation of biological materials, if the hemolysis rate is less than 5%, the material meets the requirements of hemolysis test on biological materials.

In this work we studied the concentrations of 0.138 mM, 0.690 mM, 1.380 mM, 3.450 mM and 6.900 mM (determination data would be effected when the concentration is higher than 6.900 mM). The Hemolysis ratios (%) are 2.42 ± 0.92, 4.06 ± 0.84, 2.35 ± 0.09, 1.94 ± 0.89 and 2.85 ± 1.02. The test result indicated that for all the concentrations of PAMNPs under test, the hemolysis rates were lower than 5%, which lie within the recommended value in standard ISO 10993–4. Furthermore, there are no significant difference among the hemolysis rates of all the levels ($P > 0.05$). These findings showed that the PAMNPs complied the requirements of hemolysis test on medical materials.

Plasma recalcification time. A plasma recalcification profile is a measure of the time taken for the clot formation in recalcified blood, and could serve as an indicator of the intrinsic coagulation system. The PAMNPs are considered to have no effect on the clotting time if the plasma recalcification time (PRT) is 40% longer than that of the positive control, i.e. not silicified glass.

Table 1 showed that, clotting time of normal saline was 185S. As compared to the normal saline, the contrast agent at high concentration had the effect of shortening recalcification time on rabbit plasma. When the contrast agent was at the concentration of 138 mM, the recalcification time was shortened to 110S. With

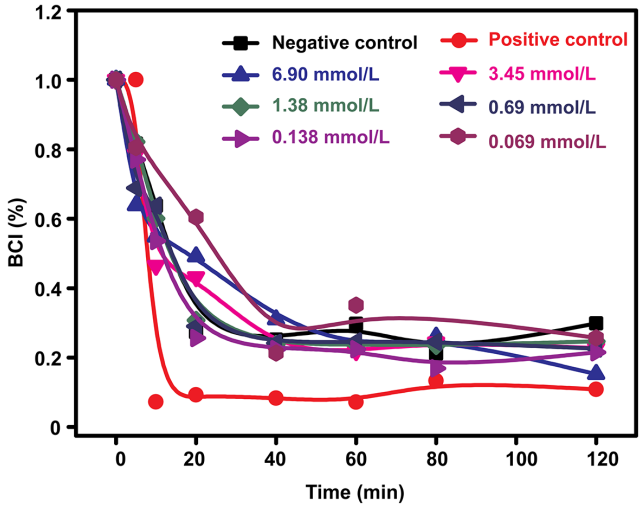

Figure 2 | Curve of dynamic clotting. The profile of positive control decreased very quickly, while the PAMNPs and the negative control decreased slowly. The curve of dynamic clotting for PAMNPs was similar to that of the negative control. The PAMNPs would not interact with fibrinogen in blood (n = 5 for each time point).

decreased concentration, this effect was reduced. When the concentration is decreased to 1.38 mM, the recalcification time was close to that of normal saline, hardly showing the effect of shortening recalcification time. When PAMNPs concentration was lower than 1.38 mM, the clotting time was basically similar to that of normal saline and the PRT was 40% longer than that of the positive control. PAMNPs did not exert a noticeable effect on the intrinsic coagulation pathway.

The result of plasma recalcification test indicated that, when PAMNPs concentration was lower than 1.38 mM, PAMNPs hardly influenced on clotting time. When the concentration was higher than 1.38 mM, they could promote activation of endogenous coagulation system and shorten the clotting time. Hence the range of concentrations of PAMNPs for safe application is recommended to be from 0 mM to 1.38 mM.

Prothrombin time (PTR). Prothrombin time means the clotting time required for platelet poor plasma, where excess tissue factors (rabbit brain effusion) are added (prothrombin is converted into thrombin). Prothrombin time test reflects the extent of activation of exogenous coagulation system.

At the customary initial concentration in blood (0.138 mM), PTR was 1.00. Table 2 had shown that, PAMNPs had the effect of reducing prothrombin time on rabbit plasma at high concentration. When the contrast agent is at the concentration of 138 mM, it's PTR was 0.57. The effect was reduced with decreased concentration. When the concentration was decreased to 7.8 mM, the effect of shortening prothrombin time was not observed, the clotting time was basically similar to that of normal saline.

Prothrombin test proved that, when the concentration of PAMNPs was below 7.80 mM, PAMNPs hardly had any effect on prothrombin time. At the concentrations above 7.80 mM, they could promote the activation of exogenous coagulation system and shorten the clotting time. The range of safe application concentration of PAMNPs is 0 mM~7.80 mM.

Dynamic clotting. Dynamic clotting time tests allow the detection of the degree of activated endogenous clotting factors.

Figure 2 exhibited the dynamic blood clotting profiles of different concentrations of PAMNPs. The time at which the absorbance equals to 0.01 is generally defined as the clotting time. The positive control showed the most rapid decrease of BCI with a whole clotting time of 10 min. All concentrations of the PAMNPs and the negative control exhibited similar BCI decrease profiles. The concentrations did not affect the BCI profiles of the PAMNPs. These data demonstrated that the PAMNPs would not interact with fibrinogen in blood.

Inflammatory cytokine release and Complement system activation. The pro-inflammatory cytokine IL-1β is involved in the initiation of inflammatory processes and contributes to inflammatory diseases. TNF-α promotes leukocyte activation and enhances the release of an array of inflammatory factors and destructive enzymes. On the hand, the complement system is an important part of the body. The decrease of C_3 level in serum may induce leukopenia decrease, immune disorder symptoms.

The extracellular content of IL-1β and TNF- α in the THP-1 cell line after 24 h of culture was shown in Figure 3. The amount of TNF-α release was similar to that of the positive control (22.5 pg/mL) (Figure 3B). For IL-1β, the release of IL-1β was also similar to that of the positive control (200 pg/mL) (Figure 3C). Thus, the effects of PAMNPs on cytokine production were significantly lower compared to the positive control, which might be attributed to an inhibitory effect of the extracts on leukocyte activation, resulting in a reduction in the release inflammatory mediators and pro-inflammatory cytokines as an amelioration of inflammation.

After incubating with serum at 37°C for 1 h, pure serum served as a negative control with the C_3 was 117.1 mg/dl, while the positive control was 290.2 mg/dl. After exposing to PAMNPs, the C_3 was similar to the negative control, and far lower than positive control (Figure 3D). It indicated the PAMNPs did not have any impact on complement system activation and possessed ideal immunological compatibility.

Toxicity to vessel. It is necessary to evaluate the toxicity of vascular because the PAMNPs are used by injection. Vascular irritation is one of the principal irritation tests to ensure clinical safe administration. In this work, we selected HUVEC cell lines to evaluate the cell toxicity.

As Figure 4A had demonstrated, after injection of PAMNPs with the maximum dose (138 mM, which is 100 times higher than working concentration), the surface of skin tissues on the dosing side of the rabbit ear is covered with squamous epithelium for both near-end and far-end of the injection site. The epithelial structure is intact and showing no keratinized hyperfunction. There was no hyperemia, edema and infiltration of inflammatory corpuscles in the mesenchyme. There was also no hyperplasia of fibrous tissue and expansion of vein lumen. At the rabbit ear region, there was no local abscission, and swelling of vascular endothelium cells. No intracavity thrombus, perivascular infiltration of lymphocytes, plasma cells, neutrophilic granulocytes and eosinophil granulocytes was observed as well.

Table 1 | Plasma recalcification time of PAMNPs (n = 5 for each time point)

Concentration (mM)	Positive control	Negative control	0.138	0.690	1.380	2.760
PRT(s)	115 ± 3	185 ± 3	185 ± 3	184 ± 4	179 ± 7	159 ± 6
Concentration (mM)	7.80	13.80	27.60	55.20	76.00	138.00
PRT(s)	151 ± 7	140 ± 9	130 ± 4	122 ± 3	118 ± 5	110 ± 3

Table 2 | Prothrombin time of PAMNPs (n = 5 for each time point)

Concentration (mM)	Control	0.138	0.69	1.38	2.76	7.80	13.80	27.60	76.00	138.00
PTR(s)	1.00	1.00	1.02	1.12	1.01	1.00	0.78	0.74	0.68	0.57

These observation were similar to the control. This proved that PAMNPs showed no obvious vascular irritation.

Figure 4B illustrated the cell viability after culture different concentrations of PAMNPs solutions for 24 h and 48 h. HUVEC cells' viability slightly varied with the incubation time and the concentration of PAMNPs ($p < 0.05$). The cell viability (%) of all groups was greater than 80%. It was noteworthy that, even with the highest concentration of 6.9 mM, the relative activity (%) was above 75%. According to the United States Pharmacopoeia Standards, it was concluded that these materials were not toxic to HUVEC cells.

According to these results, we tentatively put forward that PAMNPs could be utilized by vein injection without effects on vascula endothelial cells and vessel.

Toxicity to tissue. The former test shows that PAMNPs cause no vascular irritation. After that, the effects of PAMNPs on the other internal tissues are detected.

Tissue distribution. Contrast agents claim longer blood circulation time and easily cleared by the body. It is necessary for us to research the tissue distribution of PAMNPS.

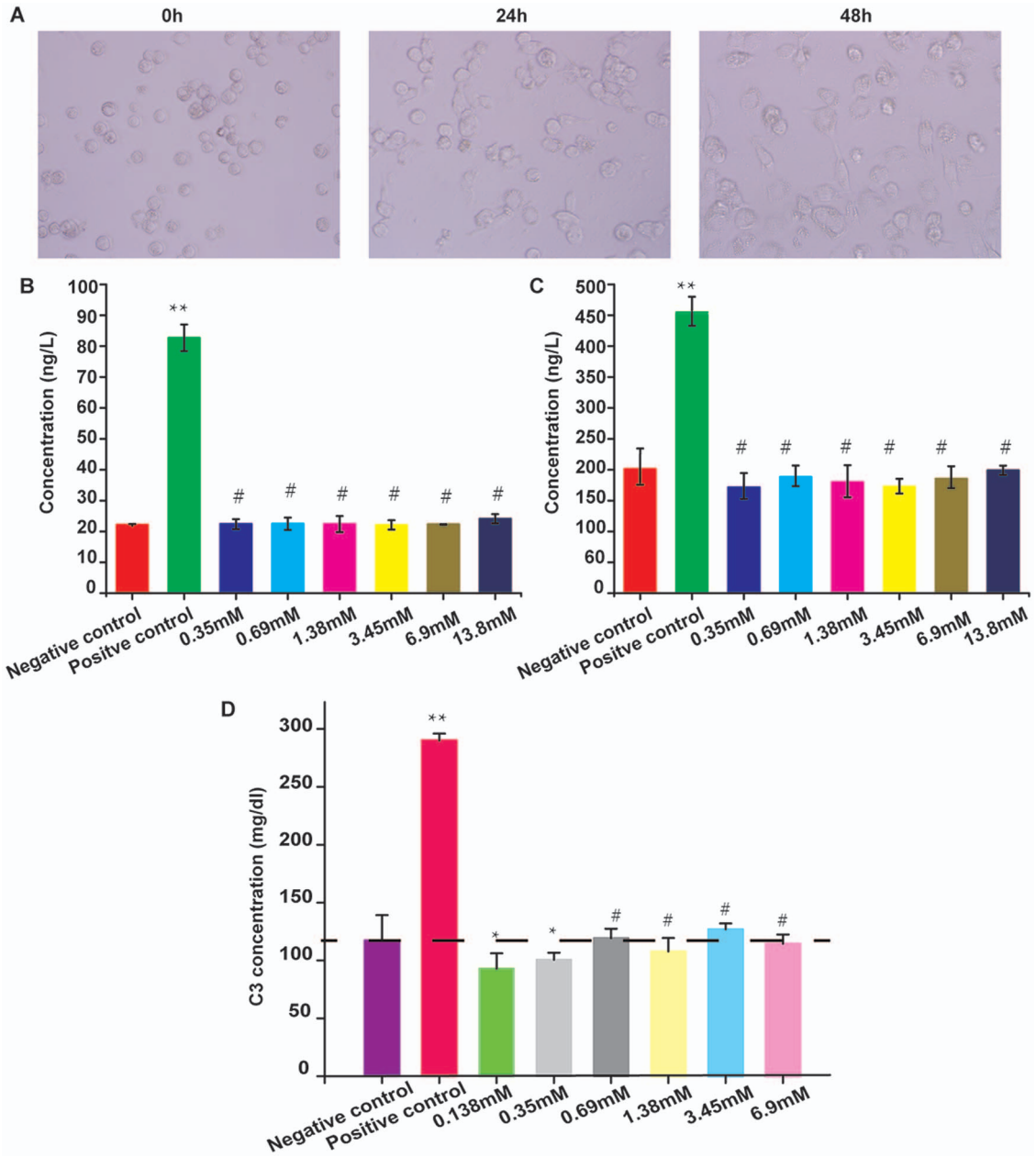

Figure 3 | PMA induced the differentiation of THP-1 cells (A), after treating for 48 hous, the THP-1 cells under went differentiation. The PAMNPs did not affect the extracellular content of TNF- α (B) and IL-1β (C) in the THP-1 cell line. The PAMNPs did not affect the concentrations of C3 left in the serum after incubated with PAMNPs either (D). (n = 3,*$p < 0.05$ and **$p < 0.01$ # $p > 0.05$ versus negative).

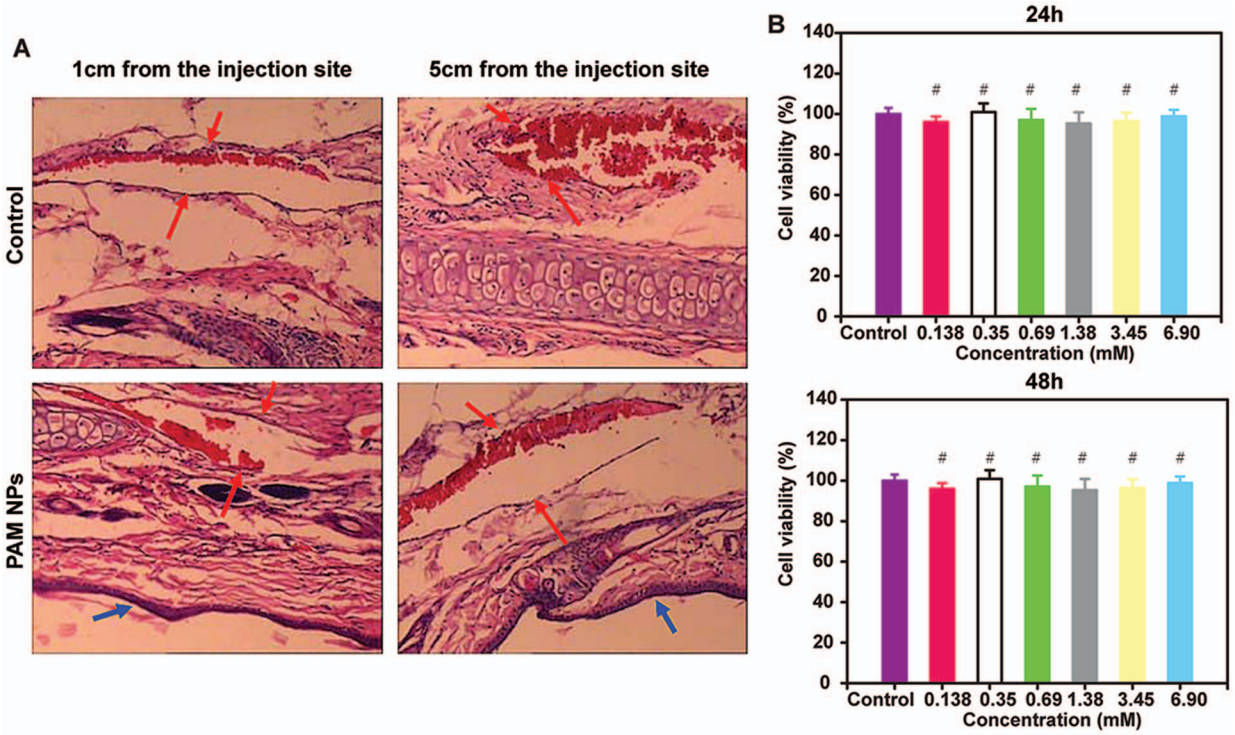

Figure 4 | (A): Representative pathology slide photomicrographs of rabbit ear vein slices. (red arrow: blood vessel; blue arrow: squamous epithelium) There was no hyperemia, edema and infiltration of inflammatory corpuscles in the mesenchyme. (B): HUVEC cell cytotoxicity of PAMNPs. There was no significant change to the cell viability of HUVEC cells. (n = 7,*p < 0.05 and **p < 0.01 # p > 0.05 versus control).

Figure 5 showed that the drug concentration in liver tissue increased rapidly, which indicated that PAMNPs could be swallowed into the liver by macrophages. Concentrations in tissues of heart, kidney, lung and spleen were relatively low. Meanwhile, PAMNPs concentration in blood was much higher than that in other tissues except liver. As a type of vascular contrast agents, PAMNPs were able to maintain a high concentration in the blood, which could provide a guarantee for its function in angiography. Activity of PAMNPs in plasma was according to the first order elimination kinetics, with the half-time in plasma being 3.77 h, and the elimination rate constant being k = 0.184. PAMNPs was higher content in plasma so as to meet the requirement of angiography. In the blood, over 99% of the internal drug could be eliminated after 7 runs of half-time.

PAMNPs could be metabolized effectively in all tissues, thus they are unlikely to pose as a hazard to organisms. The clearance rate in liver tissue was the maximum, which permited PAMNPs to be metabolized rapidly in mice bodies and cause no toxicity and adverse effects on organisms.

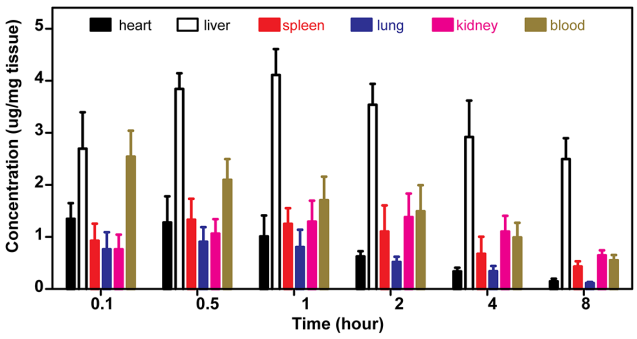

Figure 5 | **Tissue distribution of PAMNPs.** The PAMNPs almost accumulated in liver and blood. The PAMNPs were metabolized quickly in *vivo*. The half-time in plasma was 3.77 h which make it has the potential for targeting angiography. (n = 5 for each time point).

Tissue slice inspection. Results of 1.38 mM PAMNPs group were similar with control group (Figure 6). The structure of mouse heart tissue was normal, and there was no hyperemia and hydroncus in the mesenchyme, as well as no infiltration of inflammatory corpuscles such as lymphocytes, plasma cells, neutrophilic granulocytes and eosinophil granulocytes. The structure of mouse liver tissue was normal, and the structure of hepatic lobule is intact. Furthermore, the liver cells showed no swelling, degeneration, necrosis, and infiltration of inflammatory corpuscles such as lymphocytes, plasma cells and neutrophilic granulocytes, as well as no hyperplasia and expansion. The germinal center of mouse spleen also showed no proliferation, haemorrhage and infiltration of inflammatory corpuscles. A large amount of alveoli, alveolar ducts and alveolar sacs could be seen, and the alveolar space was filled with gas and shows no sigh of edema. There was also no sigh of lung congestion and infiltration of inflammatory corpuscles on top of that. The structure of the kidney was normal, and the renal tubule and renal glomerulus could be seen. The size of renal glomerulus was normal as well, and the renal tubule showed no inflammatory corpuscle and urinary cylinder.

Results of 138 mM PAMNPs group showed that the histological structures of heart, liver and kidney were normal and were similar to that of normal control mice, with the exception of slight proliferation, haemorrhage and infiltration of inflammatory corpuscles at the germinal center of the mouse spleen. Large amounts of alveoli, alveolar ducts and alveolar sacs could be seen, and the alveolar space was filled with gas without any sign of edema. Alveolar interval showed mild broadening, and alveolar epithelial cells can be seen. The lung also showed slight congestion and a little infiltration of inflammatory corpuscles.

The histological toxicity test indicatet that the mice showed no toxic symptom at normal dosing concentration (1.38 mM, 0.2 ml). When the concentration was increased by 100 times (i.e. 138 mM,

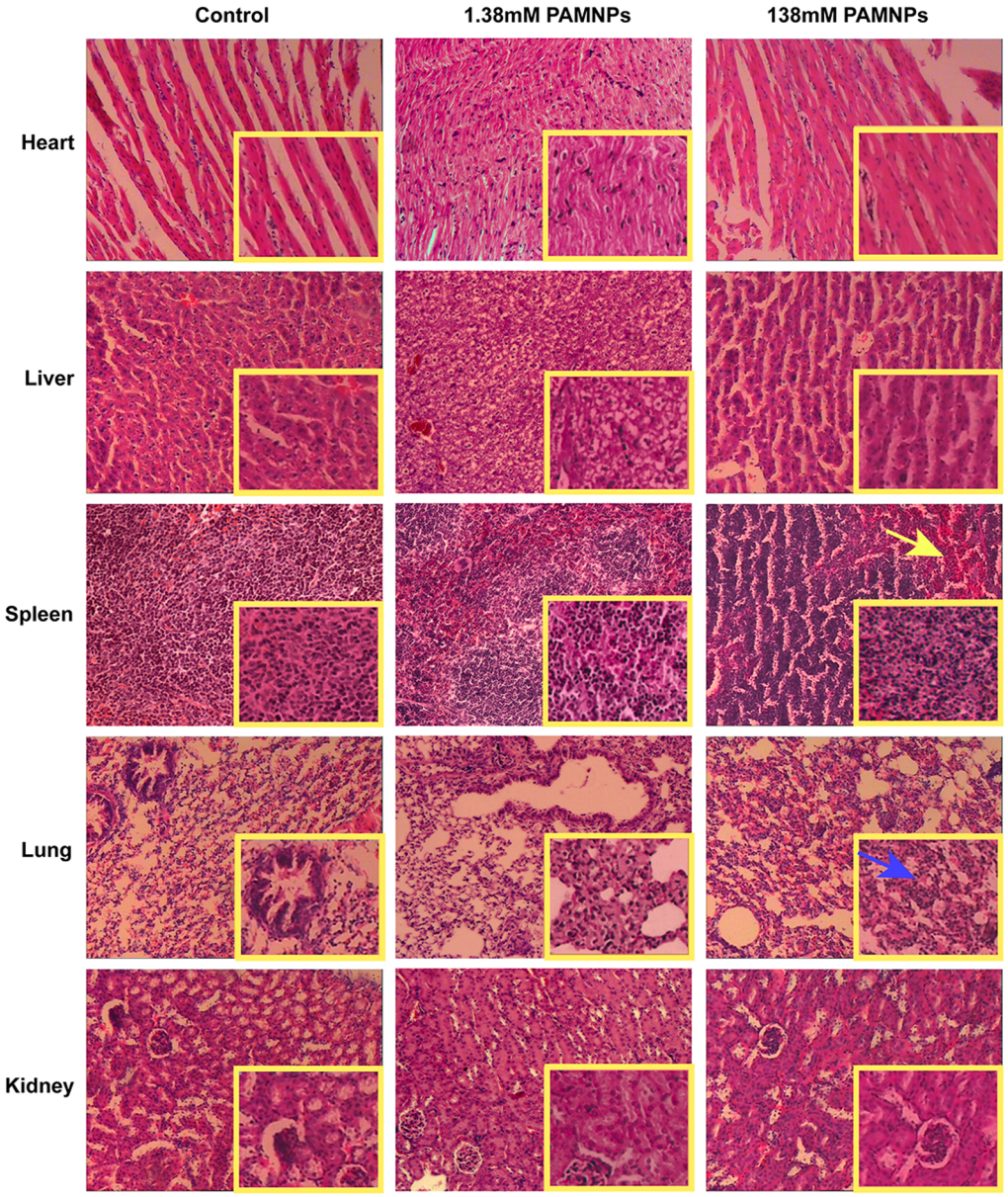

Figure 6 | Toxicity of PAMNPs to mice tissues. The histological structures of 1.38 mM group were similar with control group, while the histological structures of spleen and lung changed in 138 mM group. There were a lot of red blood cells in spleen sinus and the spleen trabecular structural were damaged (spleen: yellow arrow). The irregular blue in the interstitial showed the presence of inflammatory cell infiltration (lung: blue arrow).

0.2 ml), none of the mice died showing exceptional survival status. Pathological inspection indicated slight alteration in lung and spleen.

Results inferred that, the circulation time of PAMNPs was long enough for MRI. It could be metabolized in vivo and would cause no toxic effect to organs at the working concentration.

Conclusion

In this work, PAMNPs with a long blood circulation time were prepared based on the poly(acylic acid) (PAA)-coated magnetite nanoparticles. The purpose of this paper was to evaluate the biocompatibility of PAMNPs, providing evidence for clinical benefits.

Blood compatibility of the PAMNPs was systemically investigated by evaluating the hemolysis, plasma recalcification profiles, whole blood clotting time, prothrombin time, releasing inflammatory cytokine and complement system activation. Furthermore, toxicity to vessel and vascular cells had been tested. In addition, the biodistribution and toxicity to tissues had also been discussed.

In summary, these results suggested that the PAMNPs have excellent biocompatibility. It would not affect the hemocompatibility and have no effect on the viability of HUVEC cells. Furthermore, it would not stimulate the vascular and it showed no organ toxicity. In addition, PAMNPs had prolonged blood circulation time and could be cleared from the body. All of these benefits showed the safety of PAMNPs *in vivo*. We tentatively put forward that PAMNPs have great potential to serve as contrast agents in magnetic resonance imaging (MRI).

1. Laurent, S. *et al.* Magnetic iron oxide nanoparticles: synthesis, stabilization, vectorization, physicochemical characterizations, and biological applications. *Chem Rev* **108**, 2064–2110 (2008).
2. Reddy, L. H., Arias, J. L., Nicolas, J. & Couvreur, P. Magnetic nanoparticles: design and characterization, toxicity and biocompatibility, pharmaceutical and biomedical applications. *Chem Rev* **112**, 5818–5878 (2012).
3. Mahmoudi, M., Sant, S., Wang, B., Laurent, S. & Sen, T. Superparamagnetic iron oxide nanoparticles (SPIONs): development, surface modification and applications in chemotherapy. *Adv Drug Deliv Rev* **63**, 24–46 (2011).

4. Qiao, R., Yang, C. & Gao, M. Superparamagnetic iron oxide nanoparticles: from preparations to in vivo MRI applications. *J Mater Chem* **19**, 6274–6293 (2009).
5. Jun, Y. W., Lee, J. H. & Cheon, J. Chemical design of nanoparticle probes for high-performance magnetic resonance imaging. *Angew Chem Int Ed Engl* **47**, 5122–5135 (2008).
6. Tromsdorf, U. I., Bruns, O. T., Salmen, S. C., Beisiegel, U. & Weller, H. A highly effective, nontoxic T1 MR contrast agent based on ultrasmall PEGylated iron oxide nanoparticles. *Nano Lett* **9**, 4434–40 (2009).
7. Neuwelt, E. A. *et al.* Ultrasmall superparamagnetic iron oxides (USPIOs): a future alternative magnetic resonance (MR) contrast agent for patients at risk for nephrogenic systemic fibrosis (NSF)? *Kidney Int* **75**, 465–474 (2009).
8. Zhang, J., Rana, S., Srivastava, R. S. & Misra, R. D. On the chemical synthesis and drug delivery response of folate receptor-activated, polyethylene glycol-functionalized magnetite nanoparticles. *Acta Biomater* **4**, 40–48 (2008).
9. Kawashita, M., Kawamura, K. & Li, Z. PMMA-based bone cements containing magnetite particles for the hyperthermia of cancer. *Acta Biomater* **6**, 3187–3192 (2010).
10. Yuan, Q., Venkatasubramanian, R., Hein, S. & Misra, R. D. A stimulus-responsive magnetic nanoparticle drug carrier: magnetite encapsulated by chitosan-grafted-copolymer. *Acta Biomater* **4**, 1024–1037 (2008).
11. Ruiz, A. *et al.* Short-chain PEG molecules strongly bound to magnetic nanoparticle for MRI long circulating agents. *Acta Biomater* **9**, 6421–6430 (2013).
12. Liu, T. Y. & Huang, T. C. A novel drug vehicle capable of ultrasound-triggered release with MRI functions. *Acta Biomater* **7**, 3927–3934 (2011).
13. Zhu, A. *et al.* Polysaccharide surface modified Fe3O4 nanoparticles for camptothecin loading and release. *Acta Biomater* **5**, 1489–1498 (2009).
14. Yoo, J. W., Chambers, E. & Mitragotri, S. Factors that control the circulation time of nanoparticles in blood: challenges, solutions and future prospects. *Curr Pharm Des* **16**, 2298–2307 (2010).
15. Aggarwal, P., Hall, J. B., McLeland, C. B., Dobrovolskaia, M. A. & McNeil, S. E. Nanoparticle interaction with plasma proteins as it relates to particle biodistribution, biocompatibility and therapeutic efficacy. *Adv Drug Deliv Rev* **61**, 428–437 (2009).
16. Estephan, Z. G., Jaber, J. A. & Schlenoff, J. B. Zwitterion-stabilized silica nanoparticles: toward nonstick nano. *Langmuir* **26**, 16884–16889 (2010).
17. Estephan, Z. G., Schlenoff, P. S. & Schlenoff, J. B. Zwitteration as an alternative to PEGylation. *Langmuir* **27**, 6794–6800 (2011).
18. Chen, S., Li, L., Zhao, C. & Zheng, J. Surface hydration: principles and applications toward low-fouling/nonfouling biomaterials. *Polymer* **51**, 5283–5293 (2010).
19. Jiang, S. & Cao, Z. Ultralow-fouling, functionalizable, and hydrolyzable zwitterionic materials and their derivatives for biological applications. *Adv Mater* **22**, 920–932 (2010).
20. Petri-Fink, A., Chastellain, M., Juillerat-Jeanneret, L., Ferrari, A. & Hofmann, H. Development of functionalized superparamagnetic iron oxide nanoparticles for interaction with human cancer cells. *Biomaterials* **26**, 2685–2694 (2005).
21. Wei, H. *et al.* Compact zwitterion-coated iron oxide nanoparticles for biological applications. *Nano Lett* **12**, 22–25 (2012).
22. Wei, H., Bruns, O. T., Chen, O. & Bawendi, M. G. Compact zwitterion-coated iron oxide nanoparticles for in vitro and in vivo imaging. *Integr Biol (Camb)* **5**, 108–114 (2013).
23. Kim, D. *et al.* Facile preparation of zwitterion-stabilized superparamagnetic iron oxide nanoparticles (ZSPIONs) as an MR contrast agent for in vivo applications. *Langmuir* **28**, 9634–9639 (2012).
24. Xiao, W. C. *et al.* Microwave-assisted synthesis of magnetite nanoparticles for MR blood pool contrast agents. *J Magn Magn Mater* **324**, 488–494 (2012).
25. Xiao, W. *et al.* Prolonged in vivo circulation time by zwitterionic modification of magnetite nanoparticles for blood pool contrast agents. *Contrast Media Mol Imaging* **7**, 320–327 (2012).
26. Zhao, T., Chen, K. & Gu, H. Investigations on the interactions of proteins with polyampholyte-coated magnetite nanoparticles. *J Phys Chem B* **117**, 14129–14135 (2013).
27. Chou, F. Y., Lai, J. Y., Shih, C. M., Tsai, M. C. & Lue, S. J. In vitro biocompatibility of magnetic thermo-responsive nanohydrogel particles of poly(N-isopropylacrylamide-co-acrylic acid) with Fe3O4 cores: effect of particle size and chemical composition. *Colloids Surf B Biointerfaces* **104**, 66–74 (2013).
28. Lee, J. H. *et al.* Heparin-coated superparamagnetic iron oxide for in vivo MR imaging of human MSCs. *Biomaterials* **33**, 4861–4871 (2012).
29. Amna, T. *et al.* Electrospun Fe3O4/TiO2 hybrid nanofibers and their in vitro biocompatibility: Prospective matrix for satellite cell adhesion and cultivation. *Mat Sci Eng C-Mater* **33**, 707–713 (2013).
30. Wei, Y. *et al.* Synthesis and cellular compatibility of biomineralized Fe3O4 nanoparticles in tumor cells targeting peptides. *Colloids Surf B Biointerfaces* **107**, 180–188 (2013).
31. Wang, Q. *et al.* Pluronic-poly[alpha-(4-aminobutyl)-1-glycolic acid] polymeric micelle-like nanoparticles as carrier for drug delivery. *J Nanosci Nanotechnol* **14**, 4843–4850 (2014).
32. Wang, Q. *et al.* Uptake mechanism and endosomal fate of drug-phospholipid lipid nanoparticles in subcutaneous and in situ hepatoma. *J Biomed Nanotechnol* **10**, 993–1003 (2014).
33. Wang, Q., Qin, L., Sun, Y., Shen, M. & Duan, Y. R. Study of siRNA loaded PS-mPEG/CaP nanospheres on lung cancer. *J Nanopart Res* DOI: 10.1007/s11051-014-2421-3 (2014).
34. Li, J. *et al.* Preparation of biocompatible chitosan grafted poly(lactic acid) nanoparticles. *Int J Biol Macromol* **51**, 221–227 (2012).
35. Andrade, F. K. *et al.* Studies on the hemocompatibility of bacterial cellulose. *J Biomed Mater Res A* **98**, 554–566 (2011).
36. Wang, Q. *et al.* Preparation, blood coagulation and cell compatibility evaluation of chitosan-graft-polylactide copolymers. *Biomed Mater* **9**, 015007 (2014).
37. Wang, Q. *et al.* Preparation and properties of biocompatible PS-PEG/calcium phosphate nanospheres. *Nanotoxicology* (2014).
38. Zhang, E., Chen, H. & Shen, F. Biocorrosion properties and blood and cell compatibility of pure iron as a biodegradable biomaterial. *J Mater Sci Mater Med* **21**, 2151–2163 (2010).
39. Shenoi, R. A., Lai, B. F., Imran, U. M., Brooks, D. E. & Kizhakkedathu, J. N. Biodegradable polyglycerols with randomly distributed ketal groups as multi-functional drug delivery systems. *Biomaterials* **34**, 6068–6081 (2013).
40. Xiong, F., Xiong, C., Yao, J., Chen, X. & Gu, N. Preparation, characterization and evaluation of breviscapine lipid emulsions coated with monooleate-PEG-COOH. *Int J Pharm* **421**, 275–282 (2011).
41. She, W. *et al.* The potential of self-assembled, pH-responsive nanoparticles of mPEGylated peptide dendron-doxorubicin conjugates for cancer therapy. *Biomaterials* **34**, 1613–1623 (2013).
42. Cole, A. J., David, A. E., Wang, J., Galban, C. J. & Yang, V. C. Magnetic brain tumor targeting and biodistribution of long-circulating PEG-modified, cross-linked starch-coated iron oxide nanoparticles. *Biomaterials* **32**, 6291–6301 (2011).

Acknowledgments

This work was supported by the National Science Foundation of People's Republic of China (Nos. 81272568 and 81371542).

Author contributions

Q.W. and M.S. wrote the main manuscript text; T.Z. And Y.X. Did data collection; J.L. and M.S. participated in data analysis; Y.D. and H.G. Did study conception and design. All authors reviewed the manuscript.

Additional information

Competing financial interests: The authors declare no competing financial interests.

How to cite this article: Wang, Q. *et al.* Low toxicity and long circulation time of Polyampholyte-coated magnetic nanoparticles for blood pool contrast agents. *Sci. Rep.* **5**, 7774; DOI:10.1038/srep07774 (2015).